Investigating Local Spatially-Enhanced Structural and Textural Descriptors for Classification of iPSC Colony Images

Yulia Gizatdinova, Jyrki Rasku, Markus Haponen, Henry Joutsijoki, Ivan Baldin, Michelangelo Paci, Jari Hyttinen, Katriina Aalto-Setälä, Martti Juhola-*IEEE Member*

Abstract— **Induced pluripotent stem cells (iPSC) can be derived from fully differentiated cells of adult individuals and used to obtain any other cell type of the human body. This implies numerous prospective applications of iPSCs in regenerative medicine and drug development. In order to obtain valid cell culture, a quality control process must be applied to identify and discard abnormal iPSC colonies. Computer vision systems that analyze visual characteristics of iPSC colony health can be especially useful in automating and improving the quality control process. In this paper, we present an ongoing research that aims at the development of local spatially-enhanced descriptors for classification of iPSC colony images. For this, local oriented edges and local binary patterns are extracted from the detected colony regions and used to represent structural and textural properties of the colonies, respectively. We preliminary tested the proposed descriptors in classifying iPSCs colonies according to the degree of colony abnormality. The tests showed promising results for both, detection of iPSC colony borders and colony classification.**

I. Introduction

Induced pluripotent stem cells (iPSC) [1] can be derived from the differentiated cells of any adult individual and used to obtain different cells of the human body (e.g. neurons, functional cardiomyocytes, smooth muscle cells). The remarkable property of iPSCs to differentiate into any other cell type suggests numerous applications of iPSCs in regenerative medicine and drug development [2]. To be valid for research and therapeutic purposes, iPSCs must remain undifferentiated during culturing and passaging processes. Therefore, a continuous quality control is performed to identify and discard abnormal iPSC colonies, for example, colonies that started to differentiate spontaneously.

Visual inspection and chemical testing are currently the most common procedures to evaluate the quality of undifferentiated iPSC colonies [3]. However, man-operated visual inspection is very labor and time consuming while chemical tests can damage the colony under analysis. Computer vision, on the other hand, supports non-invasive and fully automatic approach to cell colony classification relying solely on visual characteristics of the colony health. One of the essential prerequisites for accurate colony classification is to find descriptive, robust yet fast and easy-to-compute colony representation. The current state of the art in this area includes research on wavelet features [4], various texture descriptors [3,5], and intensity histograms [6].

In this study, we concentrate on structural and textural features, namely, local oriented edges and local binary patterns. Local oriented edge (LOE) operator [7] encodes local edges of multiple orientations at different levels of image resolution. LOE operator imitates low-level pre-attentive mechanisms of visual processing in the human visual cortex [8]. Previously, LOE descriptors have been successfully applied to pattern recognition tasks [7,9]. Local binary pattern (LBP) operator [10] encodes local primitives such as points, curved lines, and spots. LBP descriptors have been used for object representation in numerous applications. It has been shown [11] that concatenated LOE-LBP histograms that combine spatial and textural image features lead to better classification performance.

The contribution of this study is twofold. Firstly, we present empirical results on the applicability of a graph-based segmentation method [12] for the task of iPSC colony border detection. Secondly, we present preliminary results of testing locally-computed spatially-enhanced LOE-LBP histograms for the task of iPSC colony representation and classification. Section 2 describes the image database, Section 3 explains the overall proposed methodology, Section 4 presents early results for both, detection of iPSC colony borders and colony classification, and, finally, Section 5 concludes the paper and describes future research.

II. Database

The database consists of 47 feeders-free iPSC colony images taken over a period of 2-10 days. The images of 1608×1208 pixel resolution were taken with Nikon Eclipse TS100 microscope, Imperx IGV-B1620M-KC000 camera, and JAI Camera Control Tool software. Image acquisition conditions differed among photographing sessions resulting into intra- and inter-image variations in magnification, lighting, sharpness, and exposure. The number and size of the colonies in the image varies; however, the colony of interest is typically located in the center of the image. In some cases, the colony is not fully visible in the image (Figure 1,*b*). The boundaries of central colonies were

Research is supported by the Council of Tampere Region under auspices of EU's European Regional Development Fund.

Y. Gizatdinova, J. Rasku, H. Joutsijoki, I. Baldin, and M. Juhola are with the School of Information Sciences, University of Tampere, Tampere, 33100 Finland, e-mail: {firstname.lastname@uta.fi}. The corresponding author's contact: +358 50 3185844; fax: +358 (0)3 2191001; e-mail: yulia.gizatdinova@uta.fi.

M. Haponen and K. Aalto-Setälä are with the Institute of Biomedical Technology, University of Tampere, e-mail: {firstname.lastname@uta.fi}.

M. Paci and J. Hyttinen are with the Department of Electronics and Communications Engineering, Tampere University of Technology, P.O. Box 527, 33101 Tampere, Finland, e-mail: {firstname.lastname@tut.fi}.

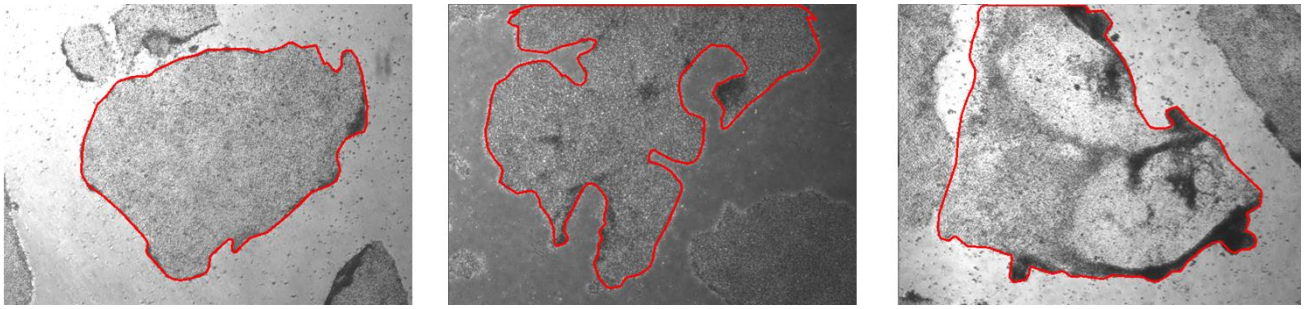

(a) (b) (c)

Figure 1. Examples of (*a*) "good", (*b*) "semigood", and (*c*) "bad" iPSC colonies with manually annotated boundaries (depicted by the red color).

manually annotated by a laboratory technician who is specialized in iPSC colony culturing. Based on visual inspection of the colonies the same specialist classified images into "good" (i.e. undifferentiated, healthy colonies without abnormalities), "semigood" (i.e. colonies with small abnormalities), and "bad" (i.e. damaged or partially differentiated colonies) categories (Figure 1). The main criteria for determining iPSC colony normality relied on the following visual characteristics: (1) translucent, homogeneous, and tight texture and intensity (e.g. absence of dark areas in the middle of the colony) and (2) distinctively sharp and near-circular shape of the colony border. In total, there are 13 images of "good", 19 images of "semigood", and 15 images of "bad" colonies in the database. For classification, the image database was divided into training set (6 "good", 7 "semigood", and 9 "bad" images) and testing set (7 "good", 8 "semigood", and 10 "bad" images).

III. Methodology

A block-diagram of the proposed classification scheme is shown in Figure 2. First, the images are converted to a gray scale representation. A graph-based segmentation method [12] is applied to divide the image into foreground and background areas (Figure 3,*b*). This method preserves detail in low-variability image regions while ignores details in high-variability regions. As recommended by the authors, we used Gaussian blur with a root mean square deviation σ=0.8 that does not produce visible changes to the image but helps to remove artifacts. Other parameters used are: k=890 to set a scale of observation and *min*=50000 to remove small segmented components. The central largest component is selected as a colony candidate. The raw segmentation mask is further dilated/eroded and processed by Canny edge detector to find the colony borders. In case of mask dilation, the resulting contour is frequently slightly larger than the manually annotated contour. The largest found contour is further smoothed by the Gaussian operator.

Next, convexity defect analysis is performed iteratively to find and split possibly merged components (Figure 3,*c*-*d*). For this, convex hull points are identified from the found contour. The resulting shape is evaluated according to several parameters which are defined empirically: (1) depth of the convexity defects, (2) distance between two points of maximal depth of convexity defects, and (3) relative size of presumably merged components. After the colony border has been detected in the image, a two-dimensional grid is constructed that divides the localized colony region into $N \times M$ separate blocks (Figure 3,*h*), where N and M are numbers of the grid columns and rows, respectively. Image features are then computed in each block of the grid and concatenated into a single feature histogram of size $N \cdot M \cdot L$ where L defines a number of histogram bins. Thus, the resulted spatially-enhanced histogram represents the distribution of local features over the whole localized colony region while preserves information about feature occurrences in different parts of the region. Grid blocks can have a certain degree of overlap which improves the classification performance [11]. Intensity, LOE, and LBP features are used in this study to form spatially-enhanced histograms of the colony regions. In contrast to differentiated "bad" colonies, undifferentiated "good" colonies contain homogeneous and tight textures, allowing us to assume that shapes of "good" colony histograms will be similar in every block of the grid while "bad" colonies will most probably reveal arbitrary distribution of features among different blocks of the grid.

The final classification is performed using two machine learning methods: multi-class AdaBoost.MH (MultiBoost) and support vector machines (SVM). MultiBoost [13] is based on a pool of simple classifiers and uses their weighted vote for final classification. Decision stumps with different weight policy are used as base classifiers. SVM [14] constructs a plane in a multi-dimensional space to separate object classes. Linear and non-linear SVM with radial basis function kernel are used. In the training phase, the classifiers learn discriminant features from the training set. The best SVM parameters C and γ are selected empirically by 10-fold cross validation procedure in a grid approach. In the testing phase, one-against-all scheme is used for classification of the testing set into the given categories.

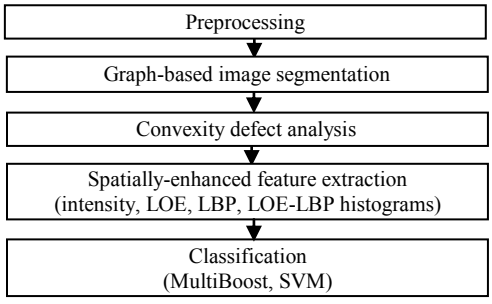

Figure 2. Block-diagram of the proposed classification scheme.

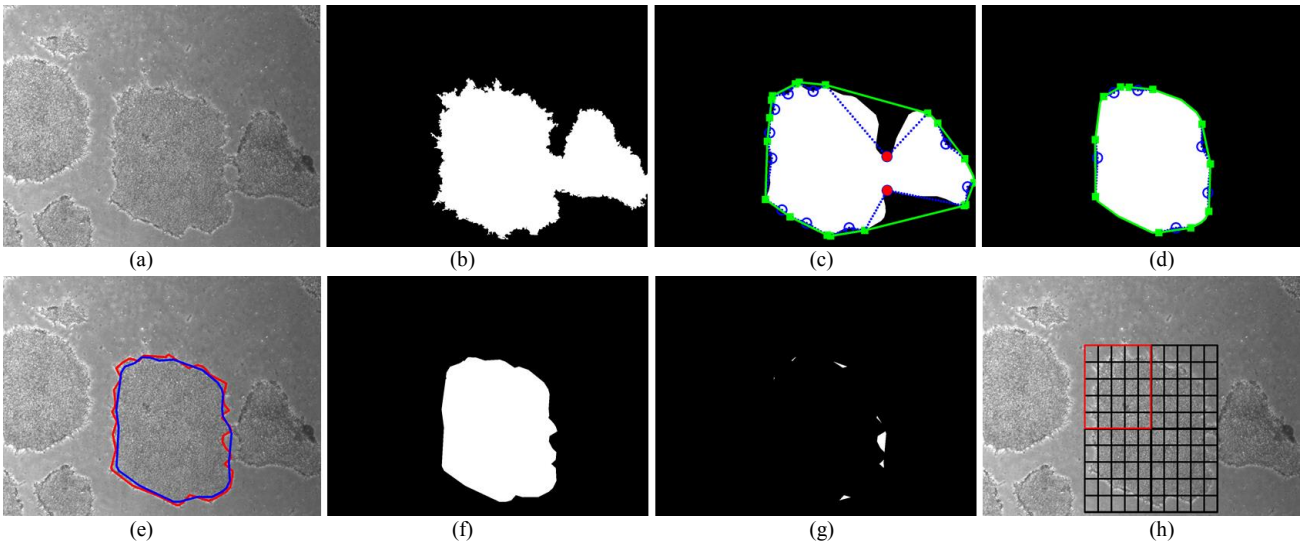

Figure 3. (*a*) "Good" iPSC colony; (*b*) raw segmentation mask; (*c-d*) convexity defect analysis iterations with convex hull (green), defect points (blue), and points of maximal depth of convexity defect (red); (*e*) manually annotated (red) and automatically detected (blue) colony borders; (*f*) useful detected area; (*g*) detected noise; and (*h*) 6×6 image grid with 80% block overlap (the size of a single block is depicted by the red color).

A. Structural and textural features

Local oriented edge (LOE) operator [7] detects structural features by convolving image pixels in a local neighbourhood. The kernels used for convolution result from differences of two Gaussians with shifted centres and encode magnitude and orientation of a local edge in the central pixel of the neighbourhood. $LOE(\varphi_k, \sigma, s, l)$ operator describes occurrences of local edges of k orientations in the colony region, where φ_k is an angle of the Gaussian rotation; s defines a pixel size of the kernel; and l is an image resolution. The length of LOE histogram is defined by k edge orientations used (Figure 4). Prior to computing LOE descriptors, the image is smoothed l times with the Gaussian filter to eliminate noise.

Local binary pattern (LBP) [10] is a texture descriptor that associates a binary code to each pixel in the image that is computed by thresholding differences between the pixel itself and surrounding pixels within a local neighborhood. $LBP(P,R)$ operator produces 2^P different binary codes that are formed by P pixels in the local circular neighbourhood of radius R. "Uniform patterns" are used to shorten the length of LBP feature vector. A combined $LOE(\varphi_k, \sigma, s, l) - LBP(P,R)$ histogram is constructed by concatenating LOE histogram to the end of LBP histogram (or wise versa) in each block of the image grid (Figure 5).

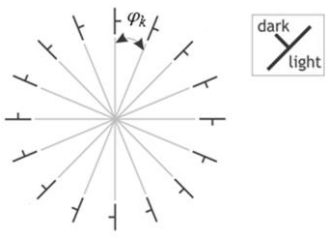

Figure 4. Example of the orientation template for calculating LOE features with $\varphi_k = k \cdot 22.5°$, $k = 0 \div 16$. Picture adapted from [7].

IV. Results and Discussion

A. Colony border detection

The automatically detected colony border S was compared against the ground truth A (i.e. manually annotated colony border). Table 1 shows performance evaluation metrics for the border detection output. In general, we used shape matching to evaluate how exactly the method detects colony borders while area metrics were utilized to evaluate mutual spatial position of A and S in the image plane.

Shape matching is based on Hu moments [15] which are invariant regarding object translation, rotation, and scale change. We used this more general metric rather than a pixel error distance between A and S because the colony boundaries were annotated by a single person; therefore, the ground truth data may contain errors and subjective decisions. Table I shows small values for the shape matching metric, meaning that in general the method was successful in finding the true shape of the colony borders.

Useful area shows the ability of the method to find image areas which are useful for the classification step (i.e. the inner part of the colony, see Figure 3,*f*). It is calculated as a ratio between the area of spatial intersection $A \cap S$ and the area of A. The average values of the useful detected area are close to 1 in Table 1, meaning that the method tends to

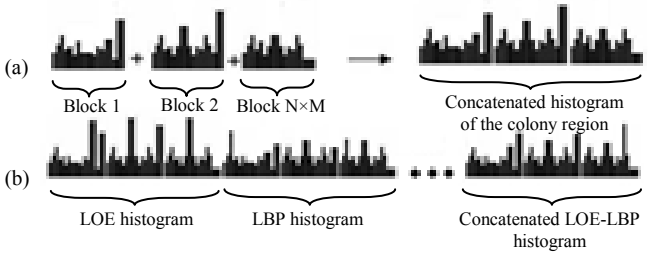

Figure 5. Construction of the spatially-enhanced concatenated LOE-LBP histogram of the image.

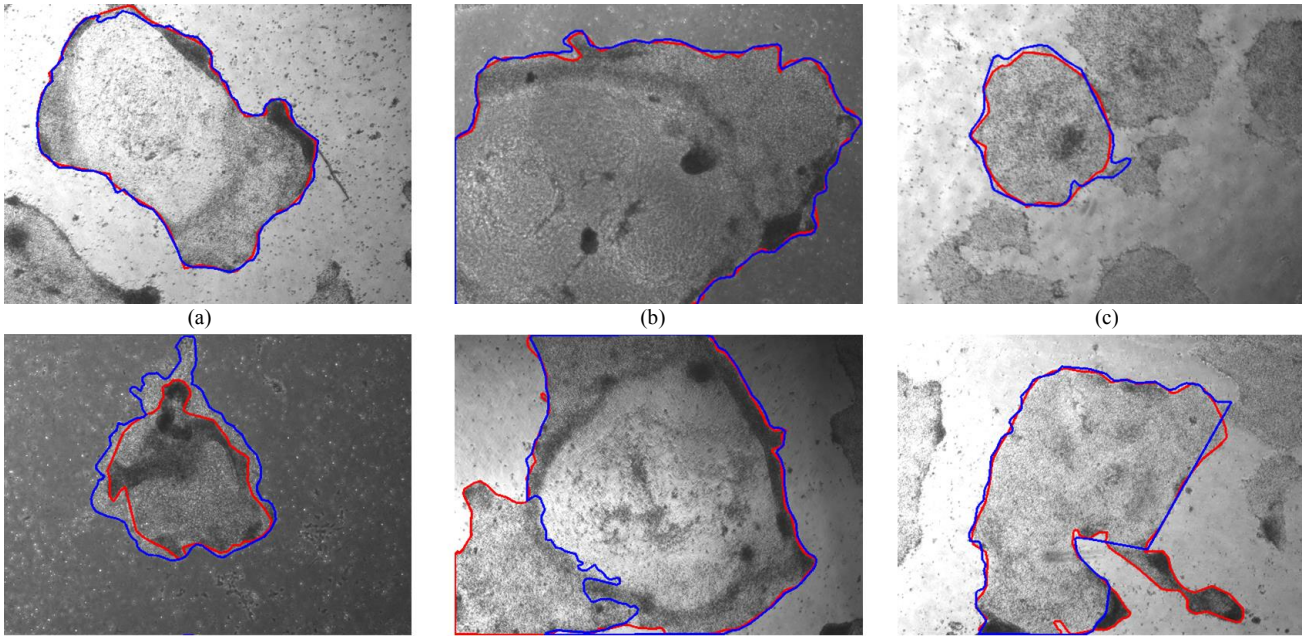

Figure 6. Examples of (*a-c*) succesful (red) and (*d-f*) wrong (blue) border detection results for "bad" iPSC colonies.

detect colonies as a whole. This is less true for "bad" colonies since they are more heterogeneous in intensity and texture as Figure 6 demonstrates.

Noise metric shows the ability of the method to discard useless image areas (i.e. neighboring colonies and culturing medium, Figure 3,*g*). It is calculated as a ratio between the detected noise and the area of *A*. This metric is rather small as Table 1 shows. The results of the colony border detection may vary depending on the parameter choice but the overall performance of the method is considered as accurate.

TABLE I. PERFORMANCE METRICS OF COLONY BORDER DETECTION

Colony category	Shape matching	Useful area	Noise
"Good"	0.07	1.00	0.12
"Bad"	0.11	0.94	0.09
"Semigood"	0.18	0.96	0.18
Total	**0.12**	**0.97**	**0.13**

B. Classification

In this study, the features were extracted from manually annotated colony regions to ensure that the classification is not affected by the errors of the colony border detection. Because the number of images used for training and testing is rather small, we report raw confusion matrices from which the reader can get an impression of the method's ability to classify images into the right category.

In overall, Multiboost classifier obtained better results than SVM classifier. Tables II-V show the best classification results obtained in different setups for intensity, LOE, LBP, and LOE-LBP spatially-enhanced histograms. Tables II-III show the results for 3-class Multiboost classification while Tables IV-V show the results for 2-class Multiboost classification. In the latter case, colony categories with some abnormalities (i.e. "semigood" and "bad") were combined into a single class.

As expected, the calculation of histograms from $N \times M$ spatial grid improved the classification results. In contrast, when the histograms were computed from the whole area of the colony, the average classification rate was not higher than 51%. However, the increase of the block amount improved the classification results only until a certain point. Thus, the most promising classification results were obtained using MultiBoost with normalized *LOE(32,0.8,5,2)* histograms on 6×6 grid with 80% block overlap (average classification rate is 80% for 3-class classification and 100% for 2-class classification). The following increase of the block amount did not improve the classification results.

V. CONCLUSIONS AND FUTURE WORK

In this paper, we presented early results from the ongoing research that aims at the development of local spatially-enhanced structural and textural descriptors for classifying iPSC colony images. It appears that MultiBoost classification with normalized *LOE(32,0.8,5,2)* histograms on 6×6 grid with 80% overlap achieved the best classification rates. However, a caution should be given to the interpretation of the current results as the image database used is rather small. More detailed research is needed to understand true abilities of the presented approach in classifying iPSC colony images.

We have identified several options for future research. First, some feature selection method will be applied to reduce the dimensionality of the obtained feature histograms and, therefore, improve their discriminative power for the classification. Second, keeping in mind that the task is to identify abnormal colonies, "bad" and "semigood" categories

TABLE II. 3-CLASS MULTIBOOST CLASSIFICATION CONFUSION MATRIXES FOR 6×6 GRID WITH 80% OVERLAP

	Intensity	***LBP(8,3)***	***LOE (16,0.8,3,2)***	***LOE (32,0.8,5,2)***	***LOE (16,0.8,3,2)-LBP(8,3)***	***LOE (32,0.8,5,2)-LBP(8,3)***
	○ ● ◒	○ ● ◒	○ ● ◒	○ ● ◒	○ ● ◒	○ ● ◒
○	**3** 1 3	**6** 1 0	**2** 1 4	7 0 0	**6** 0 1	**5** 1 1
●	0 **8** 0	1 **5** 2	2 **5** 1	0 **4** 4	1 **5** 2	1 **5** 2
◒	1 5 **4**	3 3 **4**	2 3 **5**	0 1 **9**	4 3 **3**	2 4 **4**
	R = 0.61	*R* = 0.63	*R* = 0.47	***R* = 0.80**	*R* = 0.59	*R* = 0.58

○ - "good", ● - "bad", and ◒ - "semigood" colony categories; *R* is average classification rate.

TABLE III. 3-CLASS MULTIBOOST CLASSIFICATION CONFUSION MATRIXES FOR 12×12 GRID WITH 80% OVERLAP

	Intensity	***LBP(8,3)***	***LOE (16,0.8,3,2)***	***LOE (32,0.8,5,2)***	***LOE (16,0.8,3,2)-LBP(8,3)***	***LOE (32,0.8,5,2)-LBP(8,3)***
	○ ● ◒	○ ● ◒	○ ● ◒	○ ● ◒	○ ● ◒	○ ● ◒
○	**5** 1 1	**5** 1 1	**4** 0 3	**4** 1 2	**4** 0 3	3 1 3
●	2 **5** 0	0 **5** 3	1 **7** 0	2 **2** 4	2 **5** 1	0 **6** 2
◒	2 7 **1**	1 4 **5**	2 5 **3**	4 2 **4**	1 4 **5**	2 4 **4**
	R =0.48	***R* = 0.61**	*R* = 0.58	*R* =0.41	*R* = 0.57	*R* =0. 53

○ - "good", ● - "bad", and ◒ - "semigood" colony categories; *R* is average classification rate.

TABLE IV. 2-CLASS MULTIBOOST CLASSIFICATION CONFUSION MATRIXES FOR 6×6 GRID WITH 80% OVERLAP

	Intensity	***LBP(8,3)***	***LOE (16,0.8,3,2)***	***LOE (32,0.8,5,2)***	***LOE (16,0.8,3,2)-LBP(8,3)***	***LOE (32,0.8,5,2)-LBP(8,3)***
	○ ●	○ ●	○ ●	○ ●	○ ●	○ ●
○	**3** 4	**3** 4	**0** 7	**7** 0	4 3	4 3
●	2 **16**	6 **12**	0 **18**	0 **18**	7 11	7 11
	R =0.66	*R* = 0.55	*R* = 0.50	***R* =1.00**	*R* = 0.59	*R* =0.59

○ - "good" and ● - "bad & semigood" colony categories; *R* is average classification rate.

TABLE V. 2-CLASS MULTIBOOST CLASSIFICATION CONFUSION MATRIXES FOR 12×12 GRID WITH 80% OVERLAP

	Intensity	***LBP(8,3)***	***LOE (16,0.8,3,2)***	***LOE (32,0.8,5,2)***	***LOE (16,0.8,3,2)-LBP(8,3)***	***LOE (32,0.8,5,2)-LBP(8,3)***
	○ ●	○ ●	○ ●	○ ●	○ ●	○ ●
○	**3** 4	**3** 4	**0** 7	**4** 3	3 4	2 5
●	3 15	6 **12**	0 **18**	3 **15**	4 14	2 16
	R =0.63	*R* = 0.55	*R* = 0.50	***R* =0.70**	*R* = 0.59	*R* =0.59

○ - "good" and ● - "bad & semigood" colony categories; *R* is average classification rate.

can be given more weight as compared to "good" category. Considering that the obtained results for iPSC colony border detection are rather accurate for all three colony categories, we expect that the analysis of the border's shape and sharpness can be performed and features can be calculated straight from the detected colony areas. Another extension of the proposed methodology is to perform analysis in a spatiotemporal domain similar to the previous studies [11] which proved the advantage of such approach. Thus, colony evolution can be captured over a period of time and features can be extracted from the three orthogonal planes of the received image volume. Yet another important enhancement concerns the quality and amount of images in the database. Inspired by the current results, in our future research we plan to considerably extend the image database, making it consistent with regard to image acquisition conditions.

ACKNOWLEDGMENT

The authors thank the European Regional Development Fund, the Council of Tampere Region, the Finnish Funding Agency for Innovation TEKES, Finnish Foundation for Cardiovascular Research, and Pirkanmaa Hospital District for the financial support. The authors also thank the developers of OpenCV Open Source Computer Vision Library, Multiboost, and SVM software packages. The authors thank Finnish CSC–IT Center for Science Ltd. for the allocation of computational resources.

REFERENCES

[1] K. Takahashi and S. Yamanaka, "Induction of pluripotent stem cells from mouse embryonic and adult fibroblast cultures by defined factors," *Cell*, vol. 126(4), pp.663–676, Aug 2006.

[2] M. Pekkanen-Mattila, M. Ojala, E. Kerkelä, K. Rajala, H. Skottman, and K. Aalto-Setälä, "The effect of human and mouse fibroblast feeder cells on cardiac differentiation of human pluripotent stem cells," *Stem Cells Int.*, Article ID 875059, 10 pages, 2012.

[3] N. Lowry, R. Mangoubi, M. Desai, Y. Marzouk, and P. Sammak, "Texton-based segmentation and classification of human embryonic stem cell colonies using multi-stage Bayesian level sets," in 2012 *Proc. IEEE Int. Symposium on Biomedical Imaging: From Nano to Macro*, pp. 194–197.

[4] K. Mangoubi, C. Jeffreys, A. Copeland, M. Desai, and P. Sammak, "Non-invasive image based support vector machine classification of human embryonic stem cells," in 2007 *Proc. IEEE Int. Symposium on Biomedical Imaging: From Nano to Macro*, pp. 272–276.

[5] M. Paci, L. Nanni, A. Lahti, K. Aalto-Setala, J. Hyttinen, and S. Severi, "Non-binary coding for texture descriptors in sub-cellular and stem cell image classification," *Current Bioinformatics*, vol. 8(2), pp. 208–219, 2013.

[6] H. Joutsijoki, M. Haponen, I. Baldin, J. Rasku, Y. Gizatdinova, M. Paci, J. Hyttinen, K. Aalto-Setälä, and M. Juhola, "Histogram-based classification of iPSC colony images using machine learning methods," IEEE Int. Conference on Systems, Man, and Cybernetics, 2014, accepted.

[7] Y. Gizatdinova and V. Surakka, "Feature-based detection of facial landmarks from neutral and expressive facial images," *IEEE Trans. Pattern Analysis and Machine Intelligence*, vol. 28(1), pp. 135-139, 2006.

[8] D. Marr, "Vision: A computational investigation into the human representation and processing of visual information," W.H. Freeman, Ed. San Francisco, 1982.

[9] Y. Gizatdinova and V. Surakka, "Automatic edge-based localization of facial features from images with complex facial expressions," *Pattern Recognition Letters*, vol. 31, pp. 2436–2446, 2010.

[10] T. Ojala, M. Pietikäinen, and T. Mäenpää, "Multiresolution gray-scale and rotation invariant texture classification with local binary patterns," *IEEE Trans. Pattern Analysis and Machine Intelligence*, vol. 24(7), pp. 971–987, 2002.

[11] G. Zhao, X. Huang, Y. Gizatdinova, and M. Pietikäinen, "Combining dynamic texture and structural features for speaker identification," in 2010 *Proc. ACM Multimedia 2010 Workshop on Multimedia in Forensics, Security and Intelligence*, pp. 93–98.

[12] P. Felzenszwalb and D. Huttenlocher, "Efficient graph-based image segmentation," *Int. J. of Computer Vision*, vol. 59(2), pp.167–181.

[13] D. Benbouzid, R. Busa-Fekete, N. Casagrande, F.-D. Collin, and B. Kégl, "MultiBoost: A multi-purpose boosting package," *J. of Machine Learning Research*, vol. 13, pp. 549–553, 2012.

[14] R.-E. Fan, P.-H. Chen, and C.-J. Lin, "Working set selection using second order information for training SVM," *J. of Machine Learning Research*, vol. 6, pp. 1889–1918, 2005.

[15] Hu, "Visual pattern recognition by moment invariants," *IRE Trans. on Information Theory*, vol. 8(2), pp. 179–187, 1962.